Egypt. J. Chem. **Vol. 67**, No. 10 pp. 527 - 544 (2024)

Egyptian Journal of Chemistry

http://ejchem.journals.ekb.eg/

Citharexylum Spinosum: LC-ESI-TOF-MS Analysis and Anti-Aging Evolution on D-Galactose-Induced Aging through Anti-Inflammatory, Antioxidant Activity and Regulation of the Gut Microbiota in Rats

Safaa A. Saad,[a] Howaida I. Abd-Alla,[a,*] Hanan F. Aly,[b] Nagwa M. M. Shalaby,[a] Abd El-Moneim M. Afify, [c] Hanaa F. M. Ali,[c] Nadia M. Abdel-Moein[c]

[a] *Chemistry of Natural Compounds Department, National Research Centre, Dokki 12622, Giza, Egypt*
[b] *Therapeutic Chemistry Department, National Research Centre, Dokki 12622, Giza, Egypt*
[c] *Biochemistry Department, Faculty of Agriculture, Cairo University, Egypt*

Abstract
Recently, there has been a substantial use of phytotherapy to attenuate the metabolic disorders associated with aging induced in animal model. The current research aimed to evaluate the anti-aging activity of *Citharexylum spinosum* leaves in rats' model. Six extracts of *C. spinosum* leaves were successively obtained to determine the anti-aging activity of the plant. The cytotoxicity of the six extracts was determined to identify the safe extracts that will be further used to determine their effectiveness as anti-aging in experimental animal model. The extracts *n*-hexane (*n*-Hex), *n*-hexane: benzene (*n*-Hex: Bz) and chloroform ($CHCl_3$) showed cytotoxic effects on human normal skin fibroplast cell line, however, ethyl acetate (EtOAc), *n*-butanol (*n*-BuOH) and Ethanol: H_2O 50% (EtOH: H_2O 50%) extracts were safe. Rats were injected intraperitoneal (ip) with D-galactose (100 mg/kg b.wt. /daily) for two successive months and post one month were treated (200 mg/kg b. wt./daily) by the three safe extracts; EtOAc, *n*-BuOH and EtOH: H_2O 50%. Biochemical parameters of brain derived neurotrophic factor (BDNF), interleukin-6 (IL-6) and capsular polysaccharides (CPS), neurotransmitters [noradrenaline (NA), dopamine (Dopa) and serotonin (Ser)], oxidative stress markers [malodialdehyde (MDA) and nitric oxide (NO)], nonenzymatic antioxidant of glutathione reduced (GSH) as well as histopathological examination in brain tissue were determined. Significant enhancement in all previous parameters besides, histopathological architectures of brain treated-rats were observed. EtOH: H_2O 50% extract gave a higher extraction yield percentage and anti-aging activity than the solvents with lower polarities (*n*-Hex, *n*-Hex: Bz 1:1 and $CHCl_3$). The most promising *n*-BuOH extract's profile showed the presence of variant phytoconstituents analyzed by LC-ESI-TOF-MS for the first time. Administration of *n*-BuOH may has potent ameliorating effects in revealing symptoms and delaying complication of aging that may be related to their bioactive compounds content of of phenolics and flavonoids. All extracts of *C. spinosum* leaves with the priority of *n*-BuOH has improved the disorders in inflammatory markers, CPS, neurotransmitters, oxidative stress markers, nonenzymatic activity as well as the brain architectures of aged rats. The present study showed for the first time the anti-aging activity of these extracts and their roles on brain-gut microbiota CPS.

***Keywords*:** *Citharexylum spinosum*; Capsular polysaccharides; Aging; Neurotransmitter; Nonenzymatic antioxidant; Histopathological examination; LC-ESI-TOF-MS

1. Introduction

Aging has become a worldwide social problem where by 2030, the total number of people aged 60 will increase to 1.4 billion that accounts for one-fifth of the world's population [1-3]. It includes changes that disturb the normal biological functions of management of metabolic stress resulting in the cellular response; senescence [4, 5]. This process is characterized by nine hallmarks: epigenetic alterations, genomic instability, proteostasis loss, mitochondrial dysfunction, telomere attrition, deregulated nutrient sensing, altered cellular senescence, stem cell exhaustion, and intercellular communication [4]. Moreover, aging is an irreversible process in which the behavioral capabilities and physiological activities of various organs are gradually weakened that result in cancer, cardiovascular and neurodegenerative diseases [5, 6]. In addition, it includes the changes which occur with normal brain aging such as structural, metabolic, biochemical, molecular and cellular changes [5, 7, 8]. The structural changes are both microscopic and gross changes where, the metabolic and biochemical changes include variant groups of neurotransmitter such as acetylcholine and monamines [7]. Both brain molecular and cellular changes affect mitochondria and molecules of oxidative damage, proteasome and function of lysosome, neuronal calcium homeostasis and electrophysiological regulation [7].

BDNF is a receptor that called neurotrophic tropomyosin receptor kinase fusion negative

*Corresponding author e-mail: howaida_nrc@yahoo.com.; (Howaida I. Abd-Alla).
Receive Date: 19 March 2024, Revise Date: 18 April 2024, Accept Date: 28 April 2024
DOI: 10.21608/ejchem.2024.277822.9483

(NTRK2) or Tropomyosin receptor kinase B (TrkB) showed important roles in plasticity, maintenance, differentiation and neuronal development, throughout life [8]. BDNF has direct anti-inflammatory effects on microglias. Microglias are the primary immune-competent cells that can be driven to release pro-inflammatory cytokines and protect the brain from environmental stressors. Both of normal and pathological aging result in changes in BDNF expression [9]. Two isoforms of NTRK2 are expressed in the brain: the full-length (NTRK2-FL) and the truncated form (NTRK2-T1). The brain-specific deletion in BDNF or NTRK2 induces dendritic retraction in the cortex, neuronal shrinkage, as well as cognitive and learning deficit [10]. Aging induces a pro-inflammatory phenotype and leads to chronic inflammation where, the elevated markers of inflammation such as Interleukin-6 (IL-6), a key pro-inflammatory cytokine, are associated with aging [11].

The gut flora dysbiosis affects psychiatric symptoms and brain cognition through the microbiome-gut-brain axis, in addition to, it affects the brain immune homeostasis and triggers different aging-related diseases including the neurodegenerative diseases as Alzheimer's disease and Parkinson's disease [5, 12].

Biogenic amines specifically, dopamine (DA) and serotonin (Ser) play well-defined roles in behavior and physiology [13]. Both levels of dopamine and serotonin decrease with age across species harmonic with these signaling pathways that promote healthy aging [14]. Increase in oxidative stress is significant factor contributing to aging however; the antioxidant system such as the glutathione (GSH/GSSG) system is included in aging by preserve the balance of intracellular redox [15]. Comparing to young person's; elderly persons had a low concentration of GSH and with a decrease in biosynthesis of GSH in erythrocytes [15].

Hundreds of biologically active compounds presented in plant matrix, provide promising bioactive properties for human health. In fact, attention and priority for the medicinal plants towards healthy aging have been given by the worldwide population [16]. Recent medicines could depend on natural products or their semi-synthetic derivatives [17]. The plant-derived bioactive showed biological effects as anti-inflammatory, antioxidant, and anti-aging activities so, they are promising topic in the scientific and medical communities [14].

Family *Verbenaceae* is also known as Verbain or Verbena. It contains about 3000 species in 100 genera and Citharexylum is the largest genera (comprises 115 species) [18, 19]. *Citharexylum spinosum* (known as fiddlewood) is an ornamental tree and it contains bioactive compounds such as phenolics, flavonoids, triterpenes, lignan glycosides, sterols and iridoids [18-20]. These bioactive compounds represented in gallic acid as phenolics, naringenin, quercetin, quercetrin and rutin as flavonoids, *β*-Sitosterol as sterols [18-20]. In folk medicine, *C. spinosum* has been used as diuretic, antiarthritic, antipyretic and in liver disorders [19]. It is cultivated in Egypt as a street tree besides, its usage as a drug in various tropical and subtropical regions of the world [20] Different extracts of various organs of *C. spinosum* enhance different biological activities [19].

Therefore, the current work firstly aims to investigate the efficiency of *C. spinosum* extracts to attenuate the metabolic disorders associated with aging in D-galactose (D-gal) induced rats and further identification of the effective fraction. The subsequent chemical profiling analysis has led to the identification of a range of metabolites, mostly represented by flavonoids and phenolics. The identified metabolites were detected and were correlated to the anti-aging potential, anti-inflammatory and antioxidant capacity.

2. Materials and methods

2.1. General

2.1.1. Collection and identification of plant material

In September 2021, fresh *C. spinosum* leaves were gathered from El-Orman Botanical Garden's farm, Egypt. Prof. Dr. Mohamed El-Khateeb (Professor of Ornamental Plant Taxonomy, Faculty of Agriculture, Cairo University) authenticated the plant, and plant material was stored at the Ornamental Horticulture Department Herbarium, Faculty of Agriculture, Cairo University (Egypt). The given voucher specimen for *C. spinosum* was 001359CC-000326/ 05-01-01-0031.

2.1.2. Chemicals, reagents and standards

Standards and reagents were acquired from Sigma-Aldrich, United States. Every chemical used in this investigation is analytical grade. Biosystems (Spain, Madrid Alcobendas), Sigma Chemical Company (USA, MO, St. Louis), and Biodiagnostic Company (Egypt, Cairo) were the manufacturers of all the kits. Sigma provided the standards of flavonoids and phenolic acids utilized in LC-ESI-TOF-MS. Fisher Chemical supplied the formic acid (LC grade).

2.1.3. Sample preparation

To get rid of dirt and dust, fresh *C. spinosum* leaves were first cleaned with tap water and then with distilled water. After air drying in the shade, the leaves were ground into a coarse powder and put in opaque screw-tight jars to be used later.

2.1.4. Preparation of successive extracts of C. spinosum leaves

Successive extracts of *C. spinosum* powdered leaves were prepared [21]. In ascending order of polarity, six successive solvents were used as follows: *n*-hexane (*n*-Hex), *n*-hexane: benzene 1:1 (*n*-Hex: Bz 1:1), chloroform ($CHCl_3$), EtOAc, *n*-BuOH and EtOH: H_2O 50% [21]. The powdered leaves of *C. spinosum* (1.5 kg) were soaked in *n*-Hex and placed on shaker (Heidolph UNIMAX 2010) for 24 h at 150 rpm. By using Whatman (No. 4) filter paper with a Buchner funnel, the extract was filtered and the plant residue was extracted twice more using the same volume of *n*-Hex. The combined filtrates were concentrated under vacuum at 40°C using Rotary evaporator (Heidolph Germany). After being dried, the remaining material residue of the plant was soaked in *n*-Hex: Bz, $CHCl_3$, EtOAc, *n*-BuOH and EtOH: H_2O 50% successively as described earlier.

2.2. Biological evaluation

2.2.1. In vitro studies

2.2.1.1. Cytotoxic activity test on human normal fibroblast cell line (BJ1)

Evaluation of cell viability was performed by the mitochondrial dependent reduction of yellow of 3-(4,5-dimethylthiazol-2-yl)-2,5-diphenyl tetrazolium bromide (MTT) to purple color of formazan [22]. At 100µg/ml and under the same conditions, doxorubicin was used as positive control gives 100% lethality [23]. Microplate multi-well reader (Bio-Rad Laboratories Inc., model 3350, Hercules, California, USA) was used to measure the absorbance (595 nm) and 620 nm wavelength of reference. A statistical significance was tested between the negative control and samples (vehicle with cells) using the program of independent *t*-test by SPSS 11. According to following the formula, the percentage's change in viability was calculated:

[(Reading of extract / Reading of negative control) - 1] x 100

By using SPSS 11, a probit analysis was performed to determine the IC_{50} and IC_{90}.

2.2.2. In vivo studies

2.2.2.1 Care of animal

Sixty-three male albino rats, each weighing 150±20 g were kept in The National Research Centre (NRC) animal house. Before starting experiments, the animals were placed in quarantine and given a week to get used to their surroundings. Seven of them were kept in a cage at a temperature of between 26 and 29 °C, with a set light and dark cycle and unrestricted access to food and water. The use and treatment of animals in the study was authorized by the Ethical Committee Guidelines of NRC Animal (approval No: 12411122021).

2.2.2.2. Induction of aging model

D-gal (100 mg/kg b.wt.) diluted in citrate buffer (0.01 M) was freshly prepared [24] and intraperitoneally injected once a day for two consecutive months to assess D-gal-induced aging. Rats had unrestricted access to food and water following injection. Rats were examined after two months using a behavioral test called the instructive T-maze for behavioral test.

2.2.2.3. Experimental design

Nine groups of animals were divided (seven rats/group): Group 1: control rats. Groups 2- 4: normal rats orally treated with *C. spinosum* extracts (EtOAc, *n*-BuOH extract and EtOH:H_2O 50%, respectively) at a dose 200 mg/kg b.wt. daily for one month. Group 5 was the aged group. Aged rats were used as a positive control and were classified as follows: Groups 6-8 were the aged rats orally treated for one month with 200 mg/kg b.wt. *C. spinosum* EtOAc, *n*-BuOH and EtOH:H_2O 50% extracts respectively. Groups 9: aged rats treated orally with donepezil standard drug with a dose 10 mg/kg b.wt. daily for one month [24].

2.2.2.4. Biochemical analyses

2.2.2.4.1. Collection of blood and tissue samples

Rats were fasted for 12–14 hours (overnight) after two months (for the aging group) and three months (for the aging-treated groups), blood collected from orbital plexus of eyes into a dry and clean test tube. After giving the blood 10 minutes to clot, the serum was separated using a 3000 rpm centrifuge. The separated serum was then used to analyze BDNF, IL-6, and CPS biochemically. Following blood collection, rats in each group were decapitated and their brains removed right away (a portion of the brain was preserved in 10% formalin for histopathological examination). Using an electrical homogenizer, the brain tissue was homogenized in 5-10 volumes of the suitable medium. It was then centrifuged for 15 minutes at 3000 rpm. The 10% supernatants were gathered, put in Eppendorf tubes, kept at -80°C, and measured to determine neurotransmitters including: monoamines; noradrenaline (NA), serotonin (Ser) and dopamine (Dopa), oxidative stress markers; malondialdehyde (MDA), nitric oxide (NO), nonenzymatic antioxidant level (GSH) and histopathological examination of brain tissue.

2.2.2.4.2. BDNF and IL-6 level

According to the method of Baker-Herman et al. [25], the BDNF level was determined by the MyBioSource' Rat BDNF ELISA (Enzyme-Linked Immunosorbent Assay) kit. The level of IL-6 was estimated using Quantikine ELISA Rat IL-6 Immunoassay according the method of Hirano [26].

2.2.2.4.3. Effect of C. spinosum extracts on CPS level in D-gal induced aging rats

The effect of *C. spinosum* extracts on CPS level was determined according to the method of Kasper [27] and Kasper et al. [28].

2.2.2.4.3.1. Bacterial strain, culture conditions and extraction of LPS supernatant from Bacteroides fragilis

Stock cultures of the anaerobic Gram-negative bacteria *B. fragilis* strain ATCC-23745 were sourced from Channing Laboratory in Boston, Mass. *B. fragilis* was used to extract lipopolysaccharides (LPS) using an LPS extraction kit (ab239718). The Luria broth (LBS) media plate was used to cultivate the bacteria at 37 ºC. After the bacteria were harvested, the pellets were re-suspended in cold phosphate-buffered saline. After centrifuging the bacterial pellets for 10 minutes at 2500 x g, 10 volumes of lysis buffer were added to produce lysate. For breaking aggregates of bacteria, the lysate was sonicated at 3 x 30 s, and then incubated in ice for 10 min to complete lysis. The lysate was centrifuged 10 min, 4 ºC at 2500 x g and proteinase K was added to final concentration of 0.1 mg/ml. the lysate was heated at 60 ºC for 60 min and finally centrifuged (4ºC for 10 min) at 2500 g x g (quantify LPS).

2.2.2.4.3.2. Antibodies preparation

For two weeks, the animals were immunized with intramuscular injection (three times/a week) and in the third week they given a booster injection. On each vaccination day, rats were given 10 µg of *B. fragilis* CPS in 0.1 ml of phosphate-buffered saline. Through percutaneous transthoracic cardiac puncture, aliquots of blood (0.5 ml) from each rat were extracted.

4.2.2.4.3.3. CPS determination by using ELISA kit (NB100-64513)

Figure (1) showed the LPS isolated from *B. fragilis* using this protocol was loaded onto a 4-20% gradient SDS gel. The running was at 140 V (for 55 min) before staining with Coomassie blue protein stain. Lane 1 illustrates *B. fragilis* lysate prior to proteinase K digestion. Lane 2 represents lysate after proteinase K digestion of proteins. LPS gives a characteristic ladder banding pattern in coomassie blue stained SDS-PAGE gels It is known as the 10-20 KDa carbohydrate (associated with low molecular weight proteins).

2.2.2.4.4. Determination of brain monoamines

Determination of monamines was carried out according to the method of Badawy et al. [29] Brain homogenate used for the determination of brain NA, Dopa and Ser was carried out using HPLC system, Agilent technologies 1100 series (Santa Clara, California, USA), equipped with a quaternary pump (G131A model).

2.2.2.4.5. Determination of oxidative stress markers and nonenzymatic antioxidant in brain tissue

Determination of MDA , NO and GSH in brain tissue homogenate was estimated by colorimetric test according to the method of Satoh [30], Moshage et al. [31] and Beutler et al. [32].

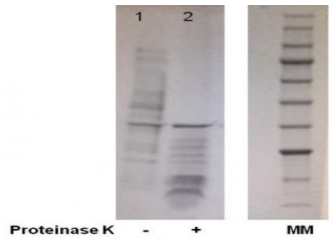

Figure 1. LPS isolated from *Bacteroides fragilis* using this protocol was loaded onto a 4-20% gradient SDS gel, run for 55 min at 140 V and then stained with Coomassie blue protein stain. LPS is a 10-20 KDa carbohydrate that is associated with low molecular weight proteins and gives a characteristic ladder banding pattern in coomassie blue stained SDS-PAGE gels. Lane 1 represents *B. fragilis* lysate prior to proteinase K digestion. Lane 2 illustrates lysate after proteinase K digestion of proteins. MM: molecular weight marker.

2.2.2.4.6. Histopathological examination of brain

Tissue samples from brain were collected from experimental groups. They were fixed in neutral buffered formalin 10%, washed, dehydrated, cleared and embedded in paraffin. Hematoxylin and Eosin was used to stain the paraffin-embedded blocks after they were sectioned at a thickness of 5 µm [33]. Stained sections were examined by a light microscope (Olympus BX50, Japan).

2.2.2.4.6.1. Histopathological lesion scoring

The following percentage was used to determine the grading of the histopathologically altered brain: no changes (0), mild (1), moderate (2) and severe (3) changes, the grading was determined by percentage as follows: <30% changes (mild change), <30% – 50% (moderate change), and >50% (severe change) [34].

2.2.3. Phytochemical Analysis

2.2.3.1. LC-ESI-TOF-MS analysis of n-BuOH extract

2.2.3.1.1. Sample preparation

A stock solution of *n*-BuOH extract was prepared from 50 mg extract dissolved in 1000 µl of the solvent mixture [H_2O: methanol (MeOH): acetonitrile (CAN) in a ratio of 2:1:1)]. The stock solution was completely dissolved using a sample vortex and ten minutes of ultrasonication at 30 kHz. After diluting an aliquot of 20 µl of the stock solution with 1000 µl of H_2O: MeOH: ACN (2:1:1) and centrifuging it for 5

minutes at 10,000 rpm, and then10 µl (1 µg/ml) was used for injection. For experiment confidence, the LC-ESI-TOF-MS analysis was also carried out on blank and quality control samples, as well as internal standard (IS). Both positive and negative modes of injection were used for the sample.

2.2.3.1.2. Instruments and acquisition method

The ExionLC system (AB Sciex, Framingham, MA, USA) was used to separate small molecules. It was connected to an autosampler system, and had an in-line filter disks pre-column (0.5 µm × 3.0 mm, Phenomenex, Torrance, CA, USA) and an Xbridge C18 (3.5 µm, 2.1 × 50 mm) column (Waters Corporation, Milford, MA, USA). The mobile phase consisted of two solutions; (A): 5 mM ammonium formate in 1% MeOH, pH adjusted to 3.0 using formic acid, and solution (B): 100% ACN for the positive mode. For the negative mode, solution (C) consisted of: 5 mM ammonium formate in 1% MeOH adjusted to pH 8 using NaOH. The following programs were used for the gradient elution: 0-20 min, 10% B; 21-25 min, 90% B; 25.01-28 min, 10% B; and finally, 90% B for column equilibration.

A Triple TOF 5600+ system with a Duo-Spray source running in the ESI mode (AB SCIEX, Concord, ON, Canada) was used for the mass spectrometry (MS) work. In the positive mode, the sprayer capillary and declustering potential voltages were 4500 and 80 eV, and in the negative mode, -4500 and -80 V. Gas 1 and gas 2 were at 40 psi, the curtain gas was at 25 psi, and the source of temperature was fixed at 600 °C. The ion tolerance of 10 ppm, the collision energies of 35 V (positive mode) and -35 V (negative mode) were employed, along with CE spreading of 20 V. The protocol, information-dependent acquisition (IDA) was used to operate the TripleTOF5600+. Analyst-TF 1.7.1 was used to create batches for the collection of MS and MS/MS data. Data from both full-scan MS and MS/MS were simultaneously gathered using the IDA technique. High-resolution survey spectra spanning from 50 to 1100 *m/z* were employed in the technique, and the mass spectrometer was set up to detect survey scans every 50 ms. Following each scan, the top 15 intense ions were chosen to obtain MS/MS fragmentation spectra [35].

2.2.3.1.3. LC-ESI-TOF-MS data processing

MS-DIAL 3.70 open-source software was used for non-targeting, small molecule comprehensive analysis of the sample [36]. ReSpect positive (2737 records) or ReSpect negative (1573 records) databases were used as reference databases based on the acquisition mode. The search parameters were set as MS1 and MS2 mass tolerance: 0.01 Da and 0.05 Da for data collection, for peak detection; minimum peak height: 100 amplitude, mass slice width: 0.05 Da, smoothing level: 2 scans, minimum peak width: 6 scans, for identification MS1 and MS2 tolerance: 0.2 Da/each, for alignment; retention time tolerance: 0.05 min and MS1 tolerance: 0.25 Da. The MS-DIAL output was utilized once more to confirm features (peaks) from the total ion chromatogram (TIC) using PeakView 2.2 and the Master View 1.1 package (AB SCIEX). The criteria used were aligned features with a Signal-to-Noise ratio greater than 5 and sample intensities: blank greater than 5.

3. Results and discussion

3.1. Extraction yield

Yield of extraction of *C. spinosum* leaves by different solvents was as following; EtOAc showed the highest percentage of yield (14.94%) followed by EtOH: H_2O 50% with percentage of 12.19%, *n*-Hex: Bz (2.50%), $CHCl_3$and (1.60%), *n*-Hex (1.20%) extract, while; *n*-BuOH extract gave the lowest yield of extraction (0.90%).

Phytochemicals are non-nutrient bioactive compounds presenting in most of the medicinal plants, fruits, vegetables, cereals and legumes [37]. Solvent polarity and concentration, temperature as well as time are the factors that affect the extraction and purification of these phytochemical substances from the plant material. Diverse phytochemicals with distinct chemical compositions are extracted using solvents with varying polarity. A single solvent cannot be used to extract every antioxidant and phytochemical presented in the plant material [38]. Increasing solvents polarity from non-polar like *n*-Hex to more polar like water is applied in successive extraction to reach the complete extraction of different compounds with different polarities [39].

The method of extracting a wide range of compounds with varying polarities involves progressively increasing the polarity of the solvents used, starting from a non-polar solvent like n-Hex and working your way up to a more polar solvent like water [40].

Ethanol is a widely used solvent for extraction, due to environmentally friendly attributes, low toxicity and easy acquisition [37]. Moreover, the percentage extraction yield increased with increasing the polarities of the solvent used where, the larger solvent volume dissolves constituents more effectively resulting in the increase of extraction yield [37]. According to the present results, EtOH: H_2O 50% extract gave a higher extraction yield percentage than the solvents with lower polarities (*n*-Hex, *n*-Hex: Bz and $CHCl_3$). In addition, the six successive extracts in the current research differentiated in the extract yield percentage. This obtained difference may rely on the chemical characteristics of the extracted molecules, the physicochemical properties of the solvents used and particularly their polarity that affects the solubility of the sample chemical constituents [41]. However, *n*-BuOH extract gave the lowest extraction yield

(0.90%). These results are parallel with the results of Allam [42].

3.2. In vitro studies

Our recent study [43] revealed that, the anticholinesterase efficacy of *C. spinosum* extracts. *n*-BuOH extract possessed the highest anticholinesterase activity with IC_{50} (µg ml^{-1}/S.D. (±)) reached to 0.6 µg/ml followed by *n*-Hex: Bz extract (IC_{50} 0.803 µg/ml), EtOH:H_2O 50% with IC_{50} 1.864 µg/ml, $CHCl_3$ extract (2.264 µg/ml), *n*-Hex extract 3.574 µg/ml and finally, EtOAc extract with IC_{50} 4.841 µg/ml.

3.2.1. Cytotoxic activity of C. spinosum different extracts

C. spinosum extracts were tested against the normal human epithelial cell line; 1- BJ1 (normal skin fibroblast). The extracts concentration ranged between (100 to 0.78 µg/ml) using MTT assay. According the cytotoxic results (Table1), the extracts; *n*-Hex, *n*-Hex: Bz and $CHCl_3$ appeared cytotoxic effects on cell line 1-BJ1. However, the extracts; EtOAc, *n*-BuOH and EtOH: H_2O 50% showed no cytotoxic activity on the normal cells.

Table1. Cytotoxicity of *C. spinosum* different extracts

Extract	Remarks (at 100 ppm)	IC_{90} (µg/ml)	IC_{50} (µg/ml)
***n*-Hex**	44.6	66.3	100%
***n*-Hex: Bz**	72.6	116.3	73.6%
$CHCl_3$	27.2	46.7	100%
EtOAc	--------	--------	9.3%
***n*-BuOH**	--------	--------	2.8%
EtOH:H_2O 50%	--------	--------	4.8%
DMSO	--------	--------	1%
Negative control	--------	--------	0 %

IC_{50}: Lethal concentration of the sample, that causes 50%death for cells in 48 hrs, IC_{90}: Lethal concentration of the sample, that causes 90%death for cells in 48 hrs, *n*-Hex: *n*-hexane, *n*-Hex: Bz: *n*-hexane:: benzene (1:1), $CHCl_3$: chloroform, EtOAc: ethyl acetate, *n*-BuOH: *n*-butanol, EtOH:H_2O 50%: ethanol:H_2O 50%. Data are mean of three replicate in each group. Statistical analysis was carried out using SPSS computer program (version11).

The extracts; *n*-Hex, *n*-Hex: Bz and $CHCl_3$ of *C. spinosum* showed cytotoxicity on normal skin fibroplast cell line. In a parallel Allam [44], illustrated that, the isolated 1,3,6-tri-*O*-galloyl-*β*-D-glucopyranose (TGG) and methyl gallate from *C. spinosum* aerial parts stimulated the melanogenesis in B16F1 murine melanoma cells with IC_{50} 1.5 and 10.8 µM, respectively. The author related this activity to the stimulation of tyrosinase activity as in tyrosinase-related protein-2, melanogenesis and tyrosinase-related protein-1 catalyzes the conversion of dopachrome to 5,6-dihydroxyindole-2-carboxylic acid (DHICA) and DHICA oxidation, respectively. The MTT cell proliferation determination on A2780 human ovarian cell line for quercetrin and quercetin isolated from *C. spinosum* aerial parts showed moderate and significant cytotoxic activity, respectively [19].

Durantoside I was isolated from dried leaves and flowers of *C. spinosum*. Chemical reactions such as acetylation silylation and decinnamoylation were used to modify the sugar moiety of durantoside I for producing new analogues of iridoid glycoside [19] and evaluate their cytotoxicity on different cell lines monocyte/ macrophage-like cell line (P-388), HeLa (KB), human colorectal adenocarcinoma (HT-29), breast cancer (MCF-7), adenocarcinomic human alveolar basal epithelial cells, (A-549) and Atlantic Salmon kidney cell line. The authors added that, the original iridoid durantoside I possessed lower cytotoxic effect than some iridoid semi-synthetic analogs in all cell lines [19]. Of these iridoids, lamiidoside and caudatoside E exhibited the highest cytotoxicity against the human cervical cancer (HeLa) cell line. The EtOAc extract of both trunk bark and flowers of *C. spinosum* showed the highest cytotoxic property against the human cervical cancer cell line (HeLa) with IC_{50} value; 88.75 ± 2.00 and 96.00 ± 2.85 µg/ ml, respectively, and against the human lung cancer (A549) cell lines with IC_{50} value; 197.00 ± 4.25 and 188.23 ± 3.88 µg/ml, respectively [19]. The authors illustrated the cytotoxic effect due to the occurrence of methoxyl groups and their numbers. Therefore, the extracts of *C. spinosum* exhibited cytotoxic property may be due to such groups.

3.3. In vivo studies

3.3.1. BDNF and IL-6 level in rats treated with C. spinosum different extracts

An insignificant change was detected in BDNF level in normal rats treated with different fractions as compared to control (Table 2). However, aged rats showed significant decrease in BDNF level with percentage 59.34% compared to control. The three aged groups- treated with EtOAc, *n*-BuOH and EtOH: H_2O 50% extracts exhibited significant increase in BDNF level with improvement percentages 48.20, 43.17 and 39.61%, compared to standard drug (53.69%). Table (2) revealed insignificant differences in IL-6 level between control and normal rats treated with different fractions. Aged rats revealed a significant increase in IL-6 level (247.03%), as compared to control. Although, treated rats with different fractions significantly decreased IL-6 level with improvement percentages; 156.83, 188.11 and 180.45% for EtOAc, *n*-BuOH and EtOH: H_2O 50% extracts respectively comparing to standard drug (182.64%). *n*-BuOH recorded the highest potent

effect compared to drug. EtOAc, *n*-BuOH and EtOH: H_2O 50% showed no cytotoxic activity on the normal cells.

Astrocytes are crucial modulators for brain functions. Their cellular pathways in modulating plasticity and neuronal activity are different. One of these pathways is neurotrophic (family of trophic factors with functions in activity, maturation and neuronal survival) pathway that mediated by BDNF [45].

All the extracts of *C. spinosum* possessed significantly increased the reduced levels of BDNF with percentages of improvement; 48.20, 43.17 and 39.61% for EtOAc, *n*-BuOH and EtOH:H_2O 50% extracts, respectively. These results are in parallel with Mattson et al. [46], who related the decline of BDNF expression in primary brain regions in aging with the age related impairments in cognitive function. In animal studies, Albini et al. [45]

Table 2. BDNF and IL-6 levels in normal, aged and treated groups

Group	Parameters	
	BDNF (PG/Ml)	Anti-inflammatory IL-6 (PG/Ml)
Normal control	297.18±8.22[a]	60.83±3.00[a]
Normal + EtOAc	307.31±11.00[a]	55.13± 2.11[a]
% Change	3.40	9.37
Normal + *n*-BuOH	294.52±9.11 [a]	53.40±3..90[a]
% Change	0.89	12.21
Normal + EtOH:H_2O 50%	304.18±7.22 [a]	55.10±2.87[a]
% Change	2.35	9.37
Aging	120.83±5.22 [b]	211.10±11.00[b]
% Change	59.34	-247.03
Aging + EtOAc	264.10±8.11 [c]	115.70±6.87[c]
% Change	11.13	90.20
% of improvement	48.20	156.83
Aging + *n*-BuOH	249.13±11.20[c]	96.67±4.21[d]
% Change	16.16	58.91
% of improvement	43.17	188.11
Aging + EtOH:H_2O 50%	238.57±12.10[c]	101.33±4.11[d]
% Change	19.72	66.57
% of improvement	39.61	180.45
Aging + drug	280.40±10.00[ac]	100.70±5.21[d]
% Change	5.64	65.54
% of improvement	53.69	182.64

BDNF: Brain derived neurotrophic factor, **IL-6:** Interleukin-6. **EtOAc:** ethyl acetate, ***n*-BuOH:** *n*-butanol, **EtOH: H_2O 50%:** ethanol: H_2O 50%. Data are mean ±SD (7 rats/each group), SPSS computer program (version 8) was used for statistical analysis, One Way Analysis of Variance (ANOVA) coupled with Co-state computer program. Different letters are significant at $P \leq 0.05$.

declared, the increase in BDNF availability boosted cognitive performance as well as it enhanced learning, the memories formation and storage that led to a great interest in BDNF for aging research.

The current study revealed the presence of bioactive compounds including the phenolic acids (caffeic and cinnamic) and flavonoids (naringenin, quercetin and luteolin). Luteolin prevented the neuronal apoptosis throughout the mTOR/4E-BP1 (mechanistic target of rapamycin/ eIF4E binding protein 1) as well as it increased neurotrophin and synaptic factor levels like BDNF in the brain regions of diet-induced obese mice. [47] Furthermore, naringenin seems to promote BDNF level expression as well as the activation of its signaling pathway ERK-extracellular-regulated kinase /CREB/BDNF) in the cerebral cortex of naïve, transgenic or amnesic mice and in aged isoflurane exposed rats [48].

A highly pleiotropic glycoprotein factor; IL-6 has the ability to modulate adaptive and innate immunity in addition to glycolysis, oxidative phosphorylation and oxidation of fatty acid as various aspects of metabolism [49]. The extracts EtOAc, *n*-BuOH and EtOH:H_2O 50% of *C. spinosum* leaves decreased the elevated levels of IL-6 with percentages of improvement reached to 156.83, 188.11 and 180.45%, respectively. In older persons, the IL-6 high circulating levels predict onset of cognitive disability [50], and a greater probability for cognitive impairment in individuals with consistently high levels IL-6 [51]. In aged mice, Porcher et al. [2], observed higher levels of IL-6 in the hippocampus especially amongst females.

Different fractions of *C. spinosum* leaves possessed anti-inflammatory property [52]. The aqueous fraction exhibited a significant anti-inflammatory effect more potent than the reference drug [52]. The phytochemical investigation of *C. spinosum* revealed the occurrence of sterols, flavonoids and triterpenes and most of these compounds have anti-inflammatory properties [52]. Furthermore, flavonoids such as quercetin, luteolin, rutin, biflavonoids, triterpenoids and steroids produced significant anti-inflammatory activities [53]. These anti-inflammatory results are in line with other prior studies for family Verbenaceae [54, 55]. The current study revealed the presence of flavonoids such as naringenin, quercetin and luteolin. So, the anti-inflammatory effect of *C. spinosum* may be attributed to the existence of such bioactive compounds.

3.3.2. CPS level in rats treated with C. spinosum different extracts

Table (3) declared insignificant difference in CPS level between the three normal groups treated with EtOAc, *n*-BuOH and EtOH: H_2O 50% extracts and control rats. However, aged rats exhibited significant increase in CPS level by percentage 717.85% as compared to control. Treated rats with EtOAc, *n*-BuOH and EtOH:H_2O 50% extracts showed marked amelioration in CPS levels with improvement percentages 67.85, 125.00, 53.57%, respectively compared to standard drug (132.14 %). *n*-BuOH showed the highest effect of all fractions compared to reference drug.

Table 3. CPS level in normal, aged and different therapeutic groups

Group	Parameters
	CPS (µg/ml)
Normal control	0.28±0.02[a]
Normal + EtOAc	0.27±0.03[a]
% Change	3.57
Normal + *n*-BuOH	0.27±0.02[a]
% Change	3.57
Normal + EtOH:H_2O 50%	0.29±0.03[a]
% Change	3.57
Aging	2.29±0.54[b]
% Change	717.85
Aging + EtOAc	2.10±0.34[bc]
% Change	650
% of improvement	67.85
Aging + *n*-BuOH	1.94±0.43[c]
% Change	592.85
% of improvement	125.00
Aging + EtOH:H_2O 50%	2.14±0.55[bc]
% Change	664.28
% of improvement	53.57
Aging + drug	1.92±0.33[c]
% Change	585.71
% of improvement	132.14

CPS: capsular polysaccharides. **EtOAc:** ethyl acetate, ***n*-BuOH:** *n*-butanol, **EtOH: H_2O 50%:** ethanol: H_2O 50%. Data are mean ± SD (7 rats/each group), SPSS computer program (version 8) was used for statistical analysis, One Way Analysis of Variance (ANOVA) coupled with Co-state computer program. Different letters are significant at $P \leq 0.05$.

Depending on the immunomodulatory effect and biological function of bacterial polysaccharide, CPS can promote the development of T cells, activate the T cell population; Dendritic cells, or other immune cells; besides they promote functions of immune cells's and enhance their maturation [56]. *B. fragilis* (an anaerobic Gram-negative bacterium) can exhibit various kinds (A-H) of capsular polysaccharide A (PSA), among which PSA exhibits high ability of immunoregulation [57] PSA prevents fatal herpes simplex encephalitis and reduces brain stem inflammation. The last activity may be exerted through inducing the secretion of gamma-interferon (IFNγ) and IL-10 by $CD4^+$T and $CD8^+$T cells or through combination with the enteric-resident plasma blasts [58]. All extracts of *C. spinosum* enhanced the CPS level in aged rats where, the level of CPS was stimulated by EtOAc, *n*-BuOH and EtOH:H_2O 50% extracts by percentages of improvement up to 67.85, 125.00 and 64.28%, respectively. The protective role of polysaccharide antigens (like PSA) could be attributed to activate $CD4^+$ T cells with strong ability [59]. This is the first time to evaluate the role of *C. spinosum* extracts on brain-gut microbiota CPS in aged rats. Depending on the collected data on the microbiota-gut-brain axis, the gut microbes can regulate Alzheimer's disease and progression throughout affecting the microglial activity, neurotransmitter production, nerve growth and integrity of the blood-brain-barrier (BBB) [3, 12]. The research of Liu et al. [60] showed that gut microbiota have the ability to delay aging throughout reducing cognitive impairment and oxidative stress. Moreover, microbiota dysbiosis trigger the dysfunction of intestinal barrier as a result of changes in the junctions of tight [61]. As a result, lipopolysaccharide activates the toll-like receptor as a component of the cell wall of Gram negative bacteria [61]. The gut microbiota have the ability to metabolize phenolics leading to metabolites production with potential activity, which may cross the BBB after reach the systemic circulation and exert biological activities [58, 62]. Moreover, the disorders of intestinal microbiota (InM) may be improve by phenolics by influencing the function and structure of InM and inducing beneficial bacteria to produce various metabolites promoting neurotransmitters secretion and hormones. Another important role is the treatment and prevention of neurodegenerative diseases throughout affecting the relationship of gut microbes-brain [5, 63]. Phenolic may act as neurotransmitters cross the BBB (direct action) or modulating the cerebrovascular system (indirect action) [5, 60, 62]. Quercetin transformed by the gut microbiota to 3,4-dihydrophenylacetic acid (DOPAC), a metabolite of the neurotransmitter dopamine has neuroprotective, anti-inflammatory cardioprotective, and anticancer activities [64].

The current results indicated the presence of polyphenols (phenolic acids and flavonoids). Therefore, the enhancing of CPS in aged rats maybe related to such polyphenols compound [42, 62, 63].

Moreover, regulation the microbiota composition depending on phenolics, or other prebiotics and probiotics may help to setting up therapeutic intervention and help to restoring the gut equilibrium [59, 62]. Additionally, because brain dysfunctions are linked to dysbiosis of the gut microbiota, a rebalance in the composition of the microbiota may result in a full or partial reversion of neuropathologies [60, 62].

3.3.3. Monamines activity in brain of treated rats with C. spinosum different extracts

Table (4) illustrated the levels of neurotransmitters; NA, Dopa and Ser that showed insignificant difference in their levels between normal rats treated with different fractions and control. However, aged group showed significant decrease in NA, Dopa and Ser levels with percentage 44.33, 24.92 and 47.85% compared to control. Medication of aged rats with EtOAc, *n*-BuOH as well as standard drug showed insignificant change in neurotransmitters level compared to control. EtOH:H_2O 50% showed the highest improvement percentage in NA level (47.66%), while, Dopa showed the highest improvement percentage with EtOAc (29.12 %) while, Ser. recorded the potent ameliorating percent with *n*-BuOH (45.35%).

Table 4. Monamines level in normal, aged and treated groups

Group	Parameters		
	Neurotransmitters (µg/g tissue)		
	NA	Dopa	Ser
Normal control	3.00±0.11[a]	3.33±0.44[a]	2.80±0.60[a]
Normal + EtOAc	3.30±0.20[a]	3.50±0.66[a]	2.73±0.23[a]
% Change	10.00	5.10	2.50
Normal + *n*-BuOH	3.06±0.09[a]	3.36±0.77[a]	2.76±0.33[a]
% Change	2.00	0.90	1.42
Normal + EtOH:H_2O 50%	3.13±0.08[a]	3.43±0.53[a]	2.76±0.33[a]
% Change	4.33	3.00	1.42
Aging	1.67±0.04[b]	2.50±0.33[b]	1.46±0.05[b]
% Change	44.33	24.92	47.85
Aging + EtOAc	2.90±0.2[a]	3.47±0.65[a]	2.50±0.07[a]
% Change	3.33	4.20	10.71
% of improvement	41.00	29.12	37.14
Aging + *n*-BuOH	3.07±0.1[a]	3.30±0.43[a]	2.73±0.66[a]
% Change	2.33	0.90	2.50
% of improvement	46.66	24.02	45.35
Aging + EtOH:H_2O 50%	3.10±0.30[a]	3.30±0.33[a]	2.67±0.21[a]
% Change	3.33	0.90	4.64
% of improvement	47.66	24.02	43.21
Aging + drug	3.10±0.11[a]	3.60±0.22[a]	2.46±0.05[a]
% Change	3.33	8.10	12.14
% of improvement	47.66	33.03	35.71

NA: noradrenalin, **Dopa:** dopamine, **Ser:** serotonin **EtOAc:** ethyl acetate, ***n*-BuOH:** *n*-butanol, **EtOH: H_2O 50%:** ethanol: H_2O 50%. Data are mean ± SD (7 rats/each group). SPSS computer program (version 8) was used for statistical analysis, One Way Analysis of Variance (ANOVA) coupled with Co-state computer program. Different letters are significant at $P \leq 0.05$.

Aging related brain alterations include accumulative damage in cellular environment, atrophy of tissues and fluctuations in neurotransmitters level [5, 7]. Major neurotransmitter systems include monoamine (catecholamine: dopamine and norepinephrine or noradrenaline, and serotonin or indole amine), and cholinergic systems [5, 60]. Dopamine and noradrenaline (important neurotransmitters that related to aging) could regulate (in the adult brain) neurogenesis and synaptic plasticity [5, 42, 60].

NA level was increased by *C. spinosum* extracts (EtOAc, *n*-BuOH and EtOH:H_2O 50%), with percentages of improvement 41.00, 46.66 and 47.66%, respectively. Dopa level in aged treated rats enhanced with percentages of improvement reached to 29.12, 24.02 and 24.02%, respectively. Also, the extracts; EtOAc, *n*-BuOH and EtOH:H_2O 50% improved the Ser levels by 37.14, 45.35 and 43.21%, respectively. Our results are in concomitant with previous studies [5, 19], where D-gal caused down regulation of both dopamine and serotonin.

Flavonoids have neurodegenerative effects [5, 42, 62, 63]. Quercetin is one of the most important agents in the field of neuro-degeneration followed by hesperetin or hesperidin, apigenin and naringenin (with similar scores) as well as taxifolin and kaempferol [5, 62, 65].

Table 5. Oxidative stress markers and nonenzymatic antioxidant activity in normal, aged and treated groups

Group	Parameters		
	MDA (nmol/g.tissue)	NO (µmol/L)	GSH (mg/g.tissue)
Normal control	4.27±0.46[a]	60.36±4.10[a]	98.75±5.00[a]
Normal + EtOAc	4.62±0.08[a]	66.33±4.12[a]	156.36±6.00[b]
% Change	8.19	9.89	58.33
Normal + *n*-BuOH	4.30±0.06[a]	61.18±3.22[a]	182.00±12.90[c]
% Change	0.70	1.35	84.30
Normal + EtOH: H_2O 50%	4.41±0.33[a]	62.80±2.54[a]	170.33±10.00[b]
% Change	3.27	4.04	72.48
Aging	7.76±0.71[b]	92.33±5.65[b]	41.14±32.20[d]
% Change	81.73	52.96	58.33
Aging + EtOAc	3.77±0.54[c]	77.02±3.21[c]	197.51±7.10[ce]
% Change	11.70	27.60	100.01
% of improvement	93.44	25.36	158.34
Aging + *n*-BuOH	3.44±0.44[c]	60.00± 2.11[a]	213.00±9.00[e]
% Change	19.43	0.59	219.59
% of improvement	101.17	53.56	174.03
Aging + EtOH: H_2O 50%	3.56±0.22[c]	68.33±5.10[ac]	193.33±8.40[ce]
% Change	16.62	13.20	95.77
% of improvement	98.36	39.76	154.11
Aging + drug	4.58±0.62[ca]	46.84±2.11[d]	185.16±5.66[c]
% Change	7.25	22.39	87.50
% of improvement	74.47	75.36	145.84

MDA: Malodialdehyde, **NO:** Nitric Oxide, **GSH:** Glutathione reduced. **EtOAc:** ethyl acetate, ***n*-BuOH:** *n*-butanol, **EtOH: H_2O 50%:** ethanol: H_2O 50%. Data are mean ±SD (7 rats/each group). SPSS computer program (version 8) was used for statistical analysis, One Way Analysis of Variance (ANOVA) combined with Co-state computer program. Different letters are significant at $P \leq 0.05$.

The current study revealed the presence of bioactive compounds including; caffeic, cinnamic, naringenin, quercetin and luteolin. Administration of quercetin (30 mg/kg) to intoxicated rats with 6-hydroxydopamine for a period of 14 consecutive days led to an amelioration in the striatal dopamine levels compared to Parkinson's disease-induced control in addition to, an observation of fewer dead neurons in the quercetin-treated group [5, 42, 62, 63]. In addition, quercetin can modulate the neurotransmitters level by inhibiting their enzymatic degradation [5, 43, 61].

Neuroprotection are exerted by antioxidant, anti-neurotoxic protein aggregates, anti-apoptotic, anti-inflammatory and pro-neurotrophic or increase the release of neurotrophic factors effects [5, 43, 63]. Different extracts of *C. spinosum* possessed anti-inflammatory and antioxidant effects [52].

The current results indicated anti-inflammatory and antioxidant of *C. spinosum* extract. Therefore, the enhancement in eurotransmitters level of the present study may be due to the presence of bioactive compounds like quercetin as well as the anti-inflammatory and antioxidant of the *C. spinosum* extracts.

3.3.4. Oxidative stress markers and nonenzymatic antioxidant in rats treated with C. spinosum different extracts

2.3.4.1. MDA and NO

Table (5) clarified the levels of MDA and NO in normal, aged and treated groups. Normal rats administrated with the extracts; EtOAc, *n*-BuOH and EtOH: H_2O 50% showed insignificant change in MDA and NO levels with percentages change; 8.19, 0.70 and 3.27%, respectively for MDA and 9.89, 1.35 and 4.04%, respectively for NO. In spite of, the aged group exhibited significant raise by percentage change; 81.73 and 52.96% for MDA and NO, respectively compared to normal rats. Rats administrated EtOAc, *n*-BuOH and EtOH: H_2O 50% extracts as well as the standard drug showed reduction in the elevated levels of MDA with improvement percentages 93.44, 101.17, 98.36 and 74.47%, respectively. Significant decrease in NO level by cure aged rats with EtOAc and drug with percentages of amelioration 25.36 and 75.36%, respectively. However, insignificant change was detected in NO level upon treated aged rats with *n*-BuOH and EtOH: H_2O 50% extracts with improvement percentages 53.56, 39.76%, respectively.

3.3.4.2. GSH

The level of GSH is presented in Table (5). Normal rats administered EtOAc, *n*-BuOH and EtOH: H_2O 50% extracts revealed significant increase in GSH level with percentages 58.33, 84.30 and 72.48%, respectively as compared to control rats. Deacresed level of GSH was detected in aged rats percentage 58.33% comparing to control rats. Amelioration in GSH level was recorded upon treatment aged rats with EtOAc, *n*-BuOH and EtOH: H_2O 50% extracts as well as standard drug with improvement percentages 158.34, 174.03, 154.11 and 145.84%, respectively. The study of Nawaz et al. [37] suggested that, in polar solvents the phytochemicals extracted are pharmaceutically more important because of the higher free radical scavenging activity value, reducing activity and antioxidant properties. *In vivo*, luteolin protects against MDA, NO and H_2O_2, as well as restoring the superoxide dismutase, glutathione S-transferase and AChE activities [5, 43, 62, 65]. Naringenin exhibited the antioxidant properties on the brain by counteracting the elevated NO and lipid peroxide levels, enhancing GSH level and inhibiting cholinesterase activity [5, 43, 63].

In agreement with previous studies [19, 64], the aerial parts of *C. spinosum* contain bioactive compounds that could encourage free radical scavenging activity. Also, in parallel with previous studies [5, 43, 63], the chloroform extract of *C. spinosum* improved the antioxidant system (GSH level, MDA and NO). Where, prophylactic and therapeutic treatment with different supplementations [praziquantel (PZQ) only and agents (vitamin E, selenium and chloroform extract of *C. quadrangular* leaves) combined with PZQ] to infected mice showed high increase in catalase (CAT), TrxR and GR activities and GSH level besides, they decreased the deviation in NO and MDA in livers compared to infected untreated mice [5, 43, 62].

For centuries, plants and their corresponding botanical preparations have been used in oxidative stress-related disorders because of their remarkable activities in both prevention and treatment of these disorders [5, 12, 16]. Neurodegenerative disorders of aging and aging-related diseases included diabetes, cancer and cardiovascular disease, which have increased exponentially, are fundamentally related to oxidative stress and redox imbalance [5, 16, 63].

Recent researches suggested that, the inhibition of the oxidative stress damage and pathological changes of the hippocampus can alleviate the cognitive impairment resulted by aging [3, 5, 61]. So, the antioxidant and anti-aging effects of *C. spinosum* extracts maybe attributed to such flavonoids.

3.4. Histopathological lesion scoring of brain in rats treated with C. spinosum different extracts

Histopathological alterations of brain were recorded and scored (Table 6) as, severe (3) moderate (2), mild (1), no changes (0) were illustrated. The grading percentage was determined as follows: >50% (severe change), <30% - 50% (moderate change), and <30% changes (mild change). [34]

Table 6. Scoring of brain histopathological alterations in normal, aged and treated groups

Lesions	Groups								
	Con	**Con + EtOAc**	**Con + *n*-BuOH**	**Con+ EtOH: H_2O 50%**	**Aging**	**Aging + EtOAc**	**Aging + *n*-BuOH**	**Aging + EtOH: H_2O 50%**	**Aging + drug**
Thickening of meningeal blood vessels	0	0	0	0	3	1	0	1	1
	0	0	0	0	3	1	1	2	2
	0	0	0	0	3	1	1	2	1
Degeneration of neurons in cerebral cortex	0	0	0	0	3	1	1	2	2
Degeneration of neurons in hippocampus	0	0	0	0	3	1	1	2	1
Degeneration of Purkinje cells in cerebellum									
Reduction in granular layer cell population in cerebellum									

Score system: score 0 = absence of the lesion in all rats of the group (n= 5), score 1= <30%, score 2= <30% – 50%, score 3= >50%. Where, Con: Control group, Con+ EtOAc: Control+ EtOAc, Con+ *n*-BuOH: Control+ *n*-BuOH, Con+ EtOH: H_2O 50%: Control+ EtOH: H_2O 50%.

Figure (2) showed the histological changes in rats' brain from normal group passing by aged to treated groups. Control rats showed normal histological structure of each hippocampus (arrow), cerebral cortex and cerebellum (Photomicrographs 1-3). In addition, normal rats treated with different extracts showed neither histopathological changes nor lesion in different brain regions (Table 6) compared to control. However, aged rats revealed degeneration of Purkinje cells (arrow), degeneration of neurons in hippocampus (arrow), great thickening in meningeal blood vessel (arrow), reduction in granular layer cell population (arrow), degeneration of neurons in cerebral cortex (arrows) and chromatolysis of cerebral neurons (arrow) (Photomicrographs 4-9).

Treatments of aged rats with *C. spinosum* EtOAc extract (Photomicrographs 10-14, Figure 2) exhibited degeneration of few neurons in hippocampus (arrow), nearly normal cerebral cortex, mild thickening in meningeal blood vessel (arrow), degeneration of few Purkinje cells (arrow) and normal granular layer cell population (arrow). Aged rats treated with *C. spinosum n*-BuOH extract (Photomicrographs 15-18) reflected the enhancement of aging disorders that represented in, nearly normal thickening of meningeal blood vessels (arrow), degeneration of few neurons in hippocampus (arrow), very few degenerated Purkinje cells in cerebellum (arrow) and few degenerated neurons in cerebral cortex (arrow). The aged group treated with EtOH: H_2O 50% extract possessed mildly thickened meningeal blood vessel (arrow), degeneration of some hippocampal neurons (arrows), degenerated Purkinje cells (arrow) and degeneration of some neurons in cerebral cortex (arrows) (Photomicrographs 19-22).

While, treated-aged rats with drug showed mild thickening in meningeal blood vessel (arrow), degeneration of few neurons in hippocampus (arrow), nearly normal granular layer cell population (arrow), degeneration of some neurons in cerebral cortex (arrows) and degeneration of some Purkinje cells (arrow) (Photomicrographs: 23-27).

All extracts of *C. spinosum* improved the disorders resulted from aging induced by D-gal. They exhibited nearly normal of cerebral cortex, granular layer cell population and thickening of meningeal blood vessels.

The present profile of *C. spinosum n*-BuOH extract revealed the presence of phenolics. Increasing evidence suggested that, the medicinal plants containing phenolics, flavonoids, and other related active substances could have anti-inflammatory, antioxidant and potentially reduce the risk of aging-related diseases including metabolic syndrome and neurodegenerative disorders [5, 43, 63, 65].

In addition, their antioxidant effects of these components against different toxins-induced aging model could be related to activation SIRT1/p53 pathway [5, 43, 63, 65].

Furthermore, plant phenolic compounds considered as an alternative tool and potential complementary for preventing and mitigating the onset and/or the progression of aging-related degenerative diseases because of their multifaceted biochemical actions [5, 63, 66]. Phenolics prevent brain aging and neurodegeneration as well as they enhance cognition and memory throughout multiple mechanisms of action [5, 65, 67]. These actions including improvement of lipid metabolism, regulation of intracellular glucose transport, increase of cerebrovascular blood flow, modulation of inner mitochondrial membrane permeability, interaction with neurotoxic heavy metals, regulation of autophagy process, toxicity/accumulation/formation

of neurotoxic proteins disruption, inhibition of microglia and astrocytes over activation, reduction of neuroinflammatory reactions, decrease of chronic oxidative stress, inhibition the activity and/or the expression of monoamine oxidases and cholinesterase enzymes, activation of synaptic signaling, stimulation of neurogenesis and inhibition of apoptosis in neurons [5, 63, 67].

The present work suggested that presence of phenolics in *C. spinosumn*-BuOH extract and the enhancements in histological investigations of brain-aged rats may be due to the occurrence of bioactive compounds.

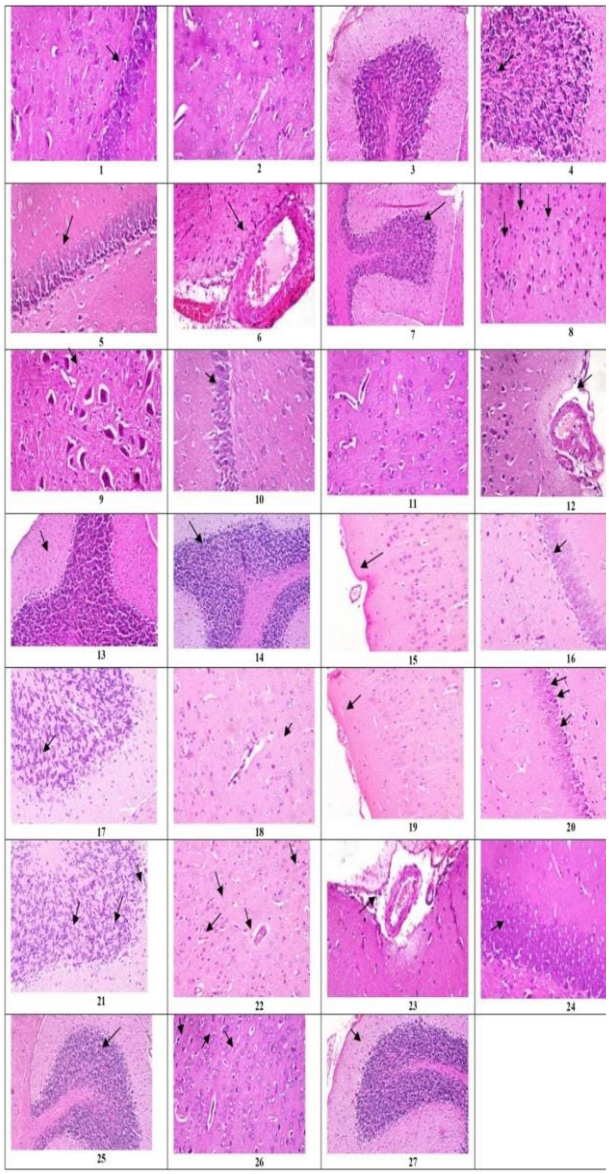

Figure 2. Histopathological investigations of rats brain in normal, aged and treated groups. Photomicrograph (1) of normal rats showing normal histological structure of hippocampus (arrow). (H&EX400). Photomicrograph (2) of normal rats showing normal histological structure of cerebral cortex (H&EX400). Photomicrograph (3) of normal rats showing normal histological structure of cerebellum (H&EX400). Photomicrograph (4) of brain of aged rats showing degeneration of Purkinje cells (arrow) (H&EX400). Photomicrograph (5) of brain of aged rats showing degeneration of degeneration of neurons in hippocampus (arrow) (H&EX400). Photomicrograph (6) of brain of aged rats showing great thickening in meningeal blood vessel (arrow) (H&EX400). Photomicrograph (7) of brain of aged rats showing reduction in granular layer cell population (arrow) (H&EX400). Photomicrograph (8) of brain of aged rats showing degeneration of neurons in cerebral cortex (arrows) (H&EX400). Photomicrograph (9) of brain of aged rats degeneration of chromatolysis of cerebral neurons (arrow) (H&EX400). Photomicrograph (10) of brain of aged rats treated with *C. spinosum* EtoAc extract showing degeneration of few neurons in hippocampus (arrow) (H&EX400). Photomicrograph (11) of brain of aged rats treated with *C. spinosum* EtoAc extract showing nearly normal cerebral cortex (H&EX400). Photomicrograph (12) of brain of aged rats treated with *C. spinosum* EtoAc extract showing mild thickening in meningeal blood vessel (arrow) (H&EX400). Photomicrograph (13) of brain of aged rats treated with *C. spinosum* EtoAc extract showing degeneration of few Purkinje cells (arrow) (H&EX400). Photomicrograph (14) of brain of aged rats treated with *C. spinosum* EtoAc extract showing and normal granular layer cell population (arrow) (H&EX400). Photomicrograph (15) of brain of aged rats treated with *C. spinosum n*-BuOH extract showing nearly normal thickening of meningeal blood vessels (arrow) (H&EX400). Photomicrograph (16) of brain of aged rats treated with *C. spinosum n*-BuOH extract showing degeneration of few neurons in hippocampus (arrow) (H&EX400). Photomicrograph (17) of brain of aged rats treated with *C. spinosum n*-BuOH extract showing very few degenerated Purkinje cells in cerebellum (arrow) (H&EX400). Photomicrograph (18) of brain of aged rats treated with *C. spinosum n*-BuOH extract showing few degenerated neurons in cerebral cortex (arrow) (H&EX400). Photomicrograph (19) of brain of aged rats treated with *C. spinosum* EtOH: H_2O extract showing mildly thickened meningeal blood vessel (arrow) (H&EX400). Photomicrograph (20) of brain of aged rats treated with *C. spinosum* EtOH: H_2O extract showing degeneration of some hippocampal neurons (arrows) (H&EX400). Photomicrograph (21) of brain of aged rats treated with *C. spinosum* EtOH: H_2O extract showing degenerated Purkinje cells (arrow) (H&EX400). Photomicrograph (22) of brain of aged rats treated with *C. spinosum* EtOH: H_2O extract showing degeneration of some neurons in cerebral cortex (arrows) (H&EX400). Photomicrograph (23) of brain of aged rats treated with drug showing mild thickening in meningeal blood vessel (arrow), (H&EX400). Photomicrograph (24) of brain of aged rats treated with drug showing mild degeneration of few neurons in hippocampus (arrow) (H&EX400). Photomicrograph (25) of brain of aged rats treated with drug showing nearly normal granular layer cell population (arrow) (H&EX400). Photomicrograph (26) of brain of aged rats treated with drug showing degeneration of some neurons in cerebral cortex (arrows) (H&EX400). Photomicrograph (27) of brain of aged rats treated with drug showing degeneration of some Purkinje cells (arrow) (H&EX400).

Table 7. Phytochemical profile of *C. spinosum n*-BuOH extract *via* LC-ESI-TOF-MS (positive mode) analysis

No.	Area %	Error	Metabolite name	R_t min.	Molecular Formula	Chemical class	Fragments or MS2 Ions *m/z*	Precursor *m/z* [M+H]+
Phenols and organic acids								
1	1.38	0.2	D-(+)-Malic acid	1.02	$C_4H_6O_5$	β-Hydroxy acids and derivatives	58.83, 71.01, 133.01	133.01
2	0.73	3.4	D-(-)-Quinic acid	27.56	$C_7H_{12}O_6$	Quinic acids and derivatives	55.01, 59.01, 190.95	190.95
3	7.44	-6.7	Caffeic acid	6.76	$C_9H_8O_4$	Hydroxy cinnamic acids	59.02, 135.04, 179.05	179.05
4	2.63	12.2	3-(4-Hydroxyphenyl) iMaleicprop-2-enoic Acid	1.70	$C_9H_8O_3$	Hydroxy cinnamic acids	51.02, 74.97, 163.04	163.04
5	3.09	8.0	*trans*-Cinnamate	11.97	$C_9H_8O_2$	Cinnamic acids	68.99, 103.05, 147.04	147.04
6	0.43	-0.3	P-Hydroxybenzoic Acid	3.92	$C_7H_6O_3$	Hydroxybenzoic acid derivatives	53.03, 75.02, 137.02	137.02
7	0.17	-0.9	E-3,4,5'-Trihydroxy-3'glucopyranosyl stilbene	1.11	$C_{20}H_{22}O_9$	Stilbene glycosides	71.01, 200.23, 405.11	405.11
Flavonoids and related metabolites								
8	0.41	14.9	Apigenin	16.97	$C_{15}H_{10}O_5$	Flavones	71.04, 125.02, 269.17	269.17
9	2.99	9.7	Isorhamnetin-3-*O*-rutinoside	8.86	$C_{28}H_{32}O_{16}$	Flavonoid-3-*O*-glycosides	59.01, 149.02, 623.19	623.19
10	0.26	7.1	Rhoifolin	8.52	$C_{27}H_{30}O_{14}$	Flavonoid-7-*O*-glycosides	291.19, 464.94, 577.13	577.13
11	0.33	6.0	Luteolin	10.76	$C_{15}H_{10}O_6$	Flavones	151.00, 270.06, 263.11	263.11
12	0.82	4.9	Acacetin	13.85	$C_{16}H_{12}O_5$	4'-*O*-Methylated flavonoids	60.99, 107.02, 283.06	283.06
13	0.74	3.2	Syringetin-3-O-galactoside	5.89	$C_{23}H_{24}O_{13}$	Flavonoid-3-*O*-glycosides	55.01, 173.03, 507.17	507.17
14	0.89	2.1	3'-Methoxy-4',5,7-trihydroxyflavonol	8.46	$C_{16}H_{12}O_7$	Flavonols	59.98, 109.00, 315.05	315.05
15	0.21	1	Baicalein-7-*O*-glucuronide	4.10	$C_{21}H_{18}O_{11}$	Flavonoid-7-*O*-glucuronides	71.00, 133.02, 445.13	445.13
16	0.05	0.2	Eriodictyol-7-*O*-neohesperidoside	6.48	$C_{27}H_{32}O_{15}$	Flavonoid-7-*O*-glycosides	56.99, 105.01, 595.16	595.16
17	9.40	0	3 5 7-trihydroxy-4'-methoxyflavone	17.04	$C_{16}H_{12}O_6$	Flavonols	59.01, 175.01, 299.20	299.20
18	0.94	-0.3	Kaempferol-7-neohesperidoside	7.79	$C_{27}H_{30}O_{15}$	Flavonoid-7-*O*-glycosides	53.18, 105.01, 593.15	593.15
19	2.22	-0.3	Quercetin-4'-glucoside	5.95	$C_{21}H_{20}O_{12}$	Flavonoid *O*-glycosides	59.01, 135.04, 463.09	463.09
20	0.07	-0.5	Quercetin-3,4'-*O*-di- β-glucopyranoside	7.16	$C_{27}H_{30}O_{17}$	Flavonoid-3-*O*-glycosides	71.00, 161.02, 625.20	625.20
21	0.05	-2.8	Acacetin-7-*O*-rutinoside	7.99	$C_{28}H_{32}O_{14}$	Flavonoid-7-*O*-glycosides	59.00, 101.02, 591.21	591.21
22	0.05	-6.2	Hesperetin	12.48	$C_{16}H_{14}O_6$	4'-*O*-methylated flavonoids	138.03, 151.03, 301.10	301.10
23	0.09	-19.4	Naringenin	1.42	$C_{15}H_{12}O_5$	Flavanones	55.01, 173.03, 271.13	271.13
24	1.79	6.6	Petunidin-3-*O*-β-glucopyranoside	7.01	$C_{22}H_{23}O_{12}$	Anthocyanidin-3-O-glycosides	71.01, 134.03, 477.10	477.10
25	23.93	-1.0	Malvidin-3-*O*-glucoside chloride	8.78	$C_{23}H_{25}O_{12}$	Anthocyanidin-3-O-glycosides	57.17, 210.29, 491.12	491.12
26	0.09	-6.3	Cyanidin-3-*O*-galactoside	6.72	$C_{21}H_{21}O_{11}$	Anthocyanidin-3-O-glycosides	71.05, 158.03, 447.10	447.10
Fatty acids								
27	0.37	0.3	2-Isopropylmalic acid	1.09	$C_7H_{12}O_5$	Hydroxy fatty acids	58.00, 73.03, 175.06	175.06
28	0.09	0.6	Citraconic acid	1.76	$C_5H_6O_4$	Methyl-branched fatty acids	55.01, 61.02, 128.96	128.96
29	0.17	-0.3	3-Hydroxy-3-Methylglutaric acid	6.37	$C_6H_{10}O_5$	Hydroxy fatty acids	55.01, 98.94, 161.02	161.02
30	8.68	-4.7	gamma-Linolenic acid	18.01	$C_{18}H_{30}O_2$	Lineolic acids and derivatives	141.09, 233.15, 277.13	277.13
Amino acids, peptides and purines								
31	0.71	2.5	Citrulline	11.03	$C_6H_{13}N_3O_3$	L-α-Amino acids	64.02, 96.00, 174.06	174.06
32	0.05	8.4	Glutathione	7.62	$C_{10}H_{17}N_3O_6S$	Peptides	67.02, 147.03, 306.09	306.09
33	0.03	0.9	Inosine	1.41	$C_{10}H_{12}N_4O_5$	Purine nucleosides	58.00, 102.99, 267.11	267.11
34	0.33	-2.3	Adenine	1.78	$C_5H_5N_5$	6-aminopurines	64.81, 92.02, 134.05	134.05
Others								
35	0.45	-14.6	Oxypurinol	8.48	$C_5H_4N_4O_2$	Xanthines	59.98, 106.02, 151.04	151.04
36	0.09	13.1	Homogenentisic acid	10.78	$C_8H_8O_4$	2(hydroxyphenyl) acetic acids	55.01, 60.98, 167.06	167.06
37	0.10	8.2	Allantoin	8.53	$C_4H_6N_4O_3$	Imidazoles	68.99, 116.95, 157.12	157.12
38	4.97	5.8	Esculin	15.71	$C_{15}H_{16}O_9$	Coumarin glycosides	149.01, 202.90, 339.11	339.11
39	0.13	5.3	D-(+)-Galacturonic acid	8.35	$C_6H_{10}O_7$	Glucuronic acid derivatives	55.01, 133.02, 193.05	193.05
40	0.27	3.7	Daphnetin	10.26	$C_9H_6O_4$	7,8-dihydroxy coumarins	117.09, 149.02, 177.01	177.01
41	0.17	2.1	Glyceric acid	1.178	$C_3H_6O_4$	Sugar acids and derivatives	58.00, 100.06, 105.07	105.07
42	0.21	1.6	Succinic acid	1.02	$C_4H_6O_4$	Dicarboxylic acids and derivatives	56.81, 73.02, 117.01	117.01
43	0.54	0.3	6,7-Dihydroxy coumarin	7.21	$C_9H_6O_4$	6,7-dihydroxy coumarins	66.00, 133.03, 177.09	177.09
44	0.10	0.3	β-Indoleacetic acid	6.99	$C_{10}H_9NO_2$	Indole-3-acetic acid derivatives	106.02, 128.05, 174.06	174.06
45	0.24	-0.3	gamma-Terpinene	1.33	$C_{10}H_{16}$	Branched unsaturated hydrocarbons	51.02, 72.98, 135.05	135.05
46	0.90	-0.7	L-Iditol	1.30	$C_6H_{14}O_6$	Sugar alcohols	51.02, 89.01, 181.07	181.07
47	0.02	-4.5	Methyl jasmonate	13.46	$C_{13}H_{20}O_3$	Jasmonic acids	74.99, 149.02, 223.14	223.14
48	0.08	-7.1	3-(4-Hydroxy-3,5-dimethoxyphenyl)-2-propenoic acid	10.09	$C_{11}H_{12}O_5$	Hydroxy cinnamic acids	56.99, 117.03, 223.06	223.06
49	0.13	-8.3	D(-)-Gulono-gamma-lactone	1.34	$C_6H_{10}O_6$	Gamma butyrolactones	55.01, 99.01, 177.04	177.04
50	0.26	-11.9	3,4-Dihydroxyphenylacetic acid	1.562	$C_8H_8O_4$	Catechols	56.99, 89.99, 166.96	166.96

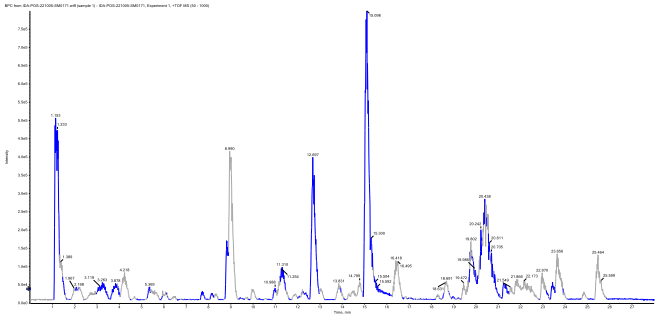

Figure 3. SM0171: Positive -MODE – BPC. The total ion chromatogram (TIC) of *C. spinosum n*-BuOH extract presented the major identified metabolites (according to the retention time) *via* LC-ESI-TOF-MS in positive ion mode.

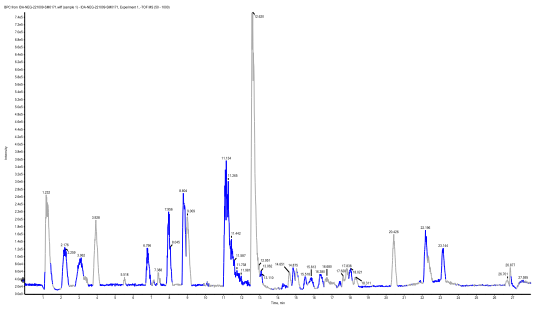

Figure 4. SM0171: Negative -MODE – BPC. The TIC of *C. spinosum n*-BuOH extract presented the major identified metabolites (according to the retention time) *via* LC-ESI-TOF-MS in negative ion mode.

Table 8. Phytochemical profiling of *C. spinosum n*-BuOH extract *via* LC-ESI-TOF-MS (negative mode) analysis

No.	Area %	Error	Metabolite name	R_t Min	Molecular Formula	Chemical class	Fragments or MS2 Ions *m/z*	Precursor *m/z* [M–H]−
Phenols and organic acids								
1	1.37	0.2	D-(+)-Malic acid	1.02	$C_4H_6O_5$	β-Hydroxy acids and derivatives	58.83, 71.01, 133.01	133.01
2	0.72	3.4	D-(-)-Quinic acid	27.56	$C_7H_{12}O_6$	Quinic acid	55.01, 119.01, 190.95	190.95
3	7.37	-6.7	Caffeic acid	6.76	$C_9H_8O_4$	Hydroxy cinnamic acids	75.96, 121.02, 179.04	179.04
4	2.60	12.2	3-(4-Hydroxyphenyl)prop-2-enoic Acid	1.70	$C_9H_8O_3$	Hydroxy cinnamic acids	51.02, 74.97, 163.04	163.04
5	3.07	8	*trans*-Cinnamate	11.97	$C_9H_8O_2$	Cinnamic acids	68.99, 103.05, 147.04	147.04
6	0.17	-0.9	E-3,4,5'-Trihydroxy-3'-glucopyranosylstilbene	1.11	$C_{20}H_{22}O_9$	Stilbene glycosides	71.01, 173.23, 405.11	405.11
7	0.43	-0.3	P-Hydroxy benzoic acid	3.92	$C_7H_6O_3$	Hydroxybenzoic acid derivatives	53.03, 95.02, 137.02	137.02
Flavonoids and related metabolites								
8	0.41	14.9	Apigenin	16.97	$C_{15}H_{10}O_5$	Flavones	71.04, 125.02, 269.17	269.17
9	2.96	9.7	Isorhamnetin-3-*O*-rutinoside	8.86	$C_{28}H_{32}O_{16}$	Flavonoid-3-*O*-glycosides	59.01, 149.02, 623.19	623.19
10	0.33	7.1	Rhoifolin	8.52	$C_{27}H_{30}O14$	Flavonoid-7-*O*-glycosides	291.19, 464.94, 577.13	577.13
11	0.23	6	Luteolin	10.76	$C_{15}H_{10}O_6$	Flavones	151.00, 270.06, 263.11	263.11
12	0.81	4.9	Acacetin	13.85	$C_{16}H_{12}O_5$	4'-*O*-methylated flavonoids	60.99, 107.02, 283.06	283.06
13	0.74	3.2	Syringetin-3-*O*-galactoside	5.89	$C_{23}H_{24}O_{13}$	Flavonoid-3-*O*-glycosides	55.01, 73.03, 507.17	507.17
14	0.88	2.1	3'-Methoxy-4',5,7-trihydroxyflavonol	8.46	$C_{16}H_{12}O_7$	Flavonols	59.98, 109.00, 315.05	315.05
15	0.18	1	Baicalein-7-*O*-glucuronide	4.10	$C_{21}H_{18}O_{11}$	Flavonoid-7-*O*-glucuronides	71.00, 133.02, 445.13	445.13
16	0.05	0.2	Eriodictyol-7-*O*-neohesperidoside	6.48	$C_{27}H_{32}O_{15}$	Flavonoid-7-*O*-glycosides	56.99, 105.01, 595.16	595.16
17	9.31	0	3,5,7-Trihydroxy-4'-methoxyflavone	17.04	$C_{16}H_{12}O_6$	Flavonols	59.01, 175.01, 299.20	299.20
18	0.93	-0.3	Kaempferol-7-neohesperidoside	7.79	$C_{27}H_{30}O_{15}$	Flavonoid-7-*O*-glycosides	53.18, 105.01, 593.15	593.15
19	2.20	-0.3	Quercetin-4'-glucoside	5.95	$C_{21}H_{20}O_{12}$	Flavonoid *O*-glycosides	59.01, 135.04, 463.09	463.09
20	0.07	-0.5	Quercetin-3,4'-O-di- β-glucopyranoside	7.16	$C_{27}H_{30}O_{17}$	Flavonoid-3-*O*-glycosides	71.00, 161.02, 625.20	625.20
21	0.06	-2.8	Acacetin-7-*O*-rutinoside	7.99	$C_{28}H_{32}O_{14}$	Flavonoid-7-*O*-glycosides	59.00, 101.02, 591.21	591.21
22	0.05	-6.2	Hesperetin	12.48	$C_{16}H_{14}O_6$	4'-*O*-methylated flavonoids	138.03, 151.03, 301.10	301.10
23	0.09	-19.4	Naringenin	1.42	$C_{15}H_{12}O_5$	Flavanones	228.07, 255.05, 271.10	271.10
24	1.78	6.6	Petunidin-3-*O*-β-glucopyranoside	7.01	$C_{22}H_{23}O_{12}$	Anthocyanidin-3-*O*-glycosides	71.01, 234.03, 477.10	477.10
25	23.71	-1	Malvidin-3-*O*-glucoside chloride	8.78	$C_{23}H_{25}O_{12}$	Anthocyanidin-3-*O*-glycosides	57.17, 210.29, 491.12	491.12
26	0.09	-6.3	Cyanidin-3-*O*-galactoside	6.72	$C_{21}H_{21}O_{11}$	Anthocyanidin-3-*O*-glycosides	71.05, 158.03, 447.10	447.10
Fatty acids								
27	0.36	0.3	2-Isopropylmalic acid	1.09	$C_7H_{12}O_5$	Hydroxy fatty acids	58.00, 73.03, 175.06	175.06
28	0.09	0.6	Citraconic acid	1.76	$C_5H_6O_4$	Methyl-branched fatty acids	55.01, 101.02, 128.96	128.96
29	0.17	-0.3	3-Hydroxy-3-methylglutaric acid	6.37	$C_6H_{10}O_5$	Hydroxy fatty acids	55.01, 98.94, 161.02	161.02
30	8.06	-4.7	gamma-Linolenic acid	18.01	$C_{18}H_{30}O_2$	Lineolic acids and derivatives	141.09, 233.15, 277.13	277.13
Amino acids, peptides and purines								
31	0.70	2.5	Citrulline	11.03	$C_6H_{13}N_3O_3$	L-α-Amino acids	64.015, 106.00, 174.06	174.06
32	0.05	8.4	Glutathione	7.62	$C_{10}H_{17}N_3O_6S$	Peptides	67.02, 147.03, 306.09	306.09
34	0.03	0.9	Inosine	1.41	$C_{10}H_{12}N_4O_5$	Purine nucleosides	58.00, 112.99, 267.11	267.11
35	0.33	-2.3	Adenine	1.78	$C_5H_5N_5$	6-Aminopurines	64.81, 92.02, 134.05	134.05
Others								
36	0.09	13.1	Homogenentisic acid	10.78	$C_8H_8O_4$	2-Hydroxyphenyl-acetic acids	55.01, 100.98, 167.06	167.06
37	4.92	5.8	Esculin	15.71	$C_{15}H_{16}O_9$	Coumarin glycosides	149.01, 202.90, 339.11	339.11
38	0.12	5.3	D-(+)-Galacturonic acid	8.35	$C_6H_{10}O_7$	Glucuronic acid derivatives	55.01, 133.02, 193.05	193.05
39	0.27	3.7	Daphnetin	10.26	$C_9H_6O_4$	7,8-dihydroxy coumarins	117.09, 149.02, 177.01	177.01
40	0.17	2.1	Glyceric acid	1.18	$C_3H_6O_4$	Sugar acids and derivatives	58.00, 85.06, 105.07	105.07
41	0.20	1.6	Succinic acid	1.02	$C_4H_6O_4$	Dicarboxylic acids and derivatives	56.81, 73.02, 117.01	117.01
42	0.22	0.4	Thymidine	8.46	$C_{10}H_{14}N_2O_5$	Pyrimidine 2'-deoxyribonucleosides	68.99, 115.03, 241.10	241.10
43	0.53	0.3	6,7-Dihydroxycoumarin	7.21	$C_9H_6O_4$	6,7-dihydroxy coumarins	66.00, 133.03, 177.09	177.09
44	0.10	0.3	β-Indoleacetic acid	6.99	$C_{10}H_9NO2$	Indole-3-acetic acid derivatives	61.02, 128.05, 174.06	174.06
45	1.11	-0.2	Sucrose	1.29	$C_{12}H_{22}O_{11}$	*O*-glycosyl compounds	55.02, 159.80, 341.11	341.11
46	0.24	-0.3	gamma-Terpinene	1.33	$C_{10}H_{16}$	Branched unsaturated hydrocarbons	51.02, 72.98, 135.05	135.05
47	0.03	-0.5	N-Acetylneuraminate	6.37	$C_{11}H_{19}NO_9$	N-acylneuraminic acids	93.02, 176.03, 308.13	308.13
48	0.89	-0.7	L-Iditol	1.30	$C_6H_{14}O_6$	Sugar alcohols	51.02, 159.01, 181.07	181.07
49	5.60	-4.4	Glucuronate	1.369	$C_6H_{10}O_7$	Glucuronic acid derivatives	51.02, 115.02, 192.07	193.07
50	0.02	-4.5	Methyl jasmonate	13.46	$C_{13}H_{20}O_3$	Jasmonic acids	74.99, 149.02, 223.14	223.14
51	0.08	-7.1	3-(4-Hydroxy-3,5-dimethoxyphenyl)-2-propenoic acid	10.09	$C_{11}H_{12}O_5$	Hydroxy cinnamic acids	56.99, 117.03, 223.06	223.06
52	0.12	-8.3	D(-)-Gulono-gamma-lactone	1.34	$C_6H_{10}O_6$	Gamma butyrolactones	55.01, 139.01, 177.04	177.04
53	0.26	-11.9	3,4-Dihydroxyphenylacetic acid	1.56	$C_8H_8O_4$	Catechols	56.99, 99.99, 166.96	166.96

3.5. Phytochemical profile of C. spinosum n-BuOH extract

LC-ESI-TOF-MS analysis of *C. spinosum n*-BuOH extract in positive (Figure 3) and negative (Figure 4) ESI mode tentatively identified 50 (Table 7) and 53 (Table 8) secondary metabolites, respectively. Different classes of metabolites were identified including phenols, flavonoids, glycosides, carboxylic acids, fatty acids, etc. (Tables 7 and 8). TIC of *C. spinosum n*-BuOH extract in positive (Figure 3) and negative (Figure 4) modes showed different classes of compounds were identified including carboxylics, phenolics and fatty acids. According to the analysis, *C. spinosum n*-BuOH extract exhibited variety of phenolic compounds such as caffeic acid (*m/z* 179.04), *trans*-cinnamate (*m/z* 147.04) and 3-(4-hydroxyphenyl) prop-2-enoic acid (*m/z* 163.04) were the major detected carboxylic acid according to area measurements and peak height. Moreover, the detected fatty acids were gamma-linolenic acid, 2-isopropylmalic acid3-hydroxy-3-methylglutaric acid, and citraconic acid at *m/z* values of 277.22, 175.06, 161.02 and128.96, respectively in both modes.

The current results of LC-MS/MS profile of *n*-BuOH extract are parallel to the study of Kamal et al. [20] Where, the chromatographic fractionation of 80% aqueous, chloroform and methanol extracts of *C. spinosum* aerial parts revealed the occurrence of flavonoid compounds (rutin, quercetrin, 6-methoxy acacetin 7-O-*β*-D-glucopyranoside, naringenin and quercetin) in addition to, gallic acid and 1,2,6-tri-*O*-galloyl-*β*-Dglucopyranoside. In addition to, the phytochemical screening of the total methanolic extract of *C. spinosum* leaves showed the presence of various metabolites including; tannins, saponins, unsaturated sterols and/or triterpenes, flavonoids, carbohydrates and/or glycosides [52]. Furthermore,

the preliminary phytochemical analysis in both of *C. spinosum* extracts (leaf and bark extract) showed the presence of triterpenoids, sterols, flavonoids, alkaloids and saponins [5, 19, 43].

The current results are matching with Saidi et al. [64]. The authors mentioned that, the phytochemical investigation for other plant parts the trunk bark ethyl acetate extract of *C. spinosum* revealed the existence of compounds including; ferulic acid, syringic acid, and vanillic acid.

All these compounds are known with their various biological activities. Thus, the antioxidant and anti-aging properties of *C. spinosum* different extracts are attributed to the occurrence of such bioactive constituents.

Conclusion

This study first time demonstrated the anti-aging, anti-inflamatory and antioxidant effects of fractionated extracts from *C. spinosum* (cultivated in Egypt). All extracts of *C. spinosum* leaves improved the disorders in inflammatory markers, CPS, neurotransmitters, oxidative stress markers, nonenzymatic activity as well as the brain architectures of aged rats that could be due to the presence of phenolics and flavonoids

4. Conflicts of interest

There are no conflicts to declare

References

[1] L. Partridge, M. Fuentealba, B. K. Kennedy, The quest to slow ageing through drug discovery, Nat. Rev. Drug Discov. 2020, 513-532.

[2] L. Porcher, S. Bruckmeier, S.D. Burbano, J.E. Finnell, N. Gorny, J. Klett, et al., Aging triggers an upregulation of a multitude of cytokines in the male and especially the

[3] female rodent hippocampus but more discrete changes in other brain regions, J. Neuroinflamm. 2021, 1-18.

[4] Z. Liu, S. Fayyaz, D. Zhao, Z. Yi, J. Huang, R. Zhou, et al., *Polygonatum sibiricum* polysaccharides improve cognitive function in D-galactose-induced aging mice by regulating the microbiota-gut-brain axis, J. Funct. Foods 2023, 1-15.

[5] S.K. Mishra, V. Balendra, J. Esposto, A.A. Obaid, R.B. Maccioni, N.K. Jha, et al., Therapeutic antiaging strategies, *Biomedicines* 2022, 1-22.

[6] P. Bellavite, Neuroprotective potentials of flavonoids: Experimental studies and mechanisms of action, *Antioxidants* 2023, 1-60.

[7] S. Moturi, S.K. Ghosh-Choudhary, T. Finkel, Cardiovascular disease and the biology of aging, J. Mol. Cell. Cardiol. 2022, 109-117.

[8] J. Lee, H.J. Kim, Normal aging induces changes in the brain and neurodegeneration progress: Review of the structural, biochemical, metabolic, cellular, and molecular changes, Front. Aging Neurosci. 2022, 1-15.

[9] H. Oh, D. Lewis, E. Sibille, The role of BDNF in age-dependent changes of excitatory and inhibitory synaptic markers in the human prefrontal cortex, Neuropsychopharmacol. 2016, 3080-3091.

[10] R.L. Simons, M.L. Ong, M.K. Lei, S.R.H. Beach, Y. Zhang, R. Philibert, et al., Changes in loneliness, BDNF, and biological aging predict trajectories in a blood-based epigenetic measure of cortical aging: A study of older black Americans, Genes (Basel) 2023) 1-14.

[11] J.A. Gorski, S.A. Balogh, J.M. Wehner, K.R. Jones, Learning deficits in forebrain-

restricted brain-derived neurotrophic factor mutant mice, Neurosci. 2003, 341-354.
[12] K.P. Loh, W. Consagra, A. Magnuson, A. Baran, N. Gilmore, S. Giri, et al., Associations of interleukin-6 with functional trajectories in older adults with cancer: Findings from the health, aging, and body composition study, Exp. Gerontol. 2023, 1-8.
[13] Y. Mou, Y. Du, L. Zhou, J. Yue, X. Hu, Y. Liu, et al., Gut microbiota interact with the brain through systemic chronic inflammation: Implications on neuroinflammation, neurodegeneration, and aging, Front. Immunol. 2022. 1-25.
[14] H.A. Miller, S. Huang, E.S. Dean, M.L. Schaller, A.M. Tuckowski, A.S. Munneke, et al., Serotonin and dopamine modulate aging in response to food odor and availability, Nat. Commun. 2022. 1-13.
[15] J.A. Yin, X. J. Liu, J. Yuan, J. Jiang, S.Q. Cai, Longevity manipulations differentially affect serotonin/dopamine level and behavioral deterioration in aging *Caenorhabditis elegans*, J. Neurosci. 2014, 3947-3958.
[16] N.T. Moldogazieva, I.M. Mokhosoev, T.I. Mel'nikova, Y.B. Porozov, A.A. Terentiev, Oxidative stress and advanced lipoxidation and glycation end products (ALEs and AGEs) in aging and age-related diseases, Oxid. Med. Cell. Longev. 2019, 1-14.
[17] H.M. Sweelam, H.I. Abd-Alla, A.B. Abdelwahab, M.M. Gabr, G. Kirsch, Secondary metabolites and biological activity of *Pentas* species: A mini review, J. Adv. Res. 2018, 21-30.
[18] J. Apisornopas, P. Silalai, T. Kasemsuk, A. Athipornchai, U. Sirion, K. Suksen, et al., Synthetic analogues of durantoside I from *Citharexylum spinosum* L. and their cytotoxic activity, Med. Chem. Lett. 2018, 1558-1561.
[19] N.Z. Mohamed, H.I. Abd-Alla, H.F. Aly, M. Mantawy, N. Ibrahim, S.A. Hassan, CCl_4-induced hepatonephrotoxicity: protective effect of nutraceuticals on inflammatory factors and antioxidative status in rat, J. Appl. Pharm. Sci. 2014, 87-100.
[20] I. Saidi, V.D. Nimbarte, H. Schwalbe, P. Waffo-Téguo, A.H. Harrath, L. Mansour, et al., Antityrosinase, anticholinesterase and cytotoxic activities of extracts and phytochemicals from the Tunisian *Citharexylum spinosum* L.: Molecular docking and SAR analysis, Bioorg. Chem. 2020, 1-11.
[21] A.M. Kamal, M.I. Abdelhady, H. Tawfeek, M.G. Haggag, E.G. Haggag, Phytochemical and biological analyses of *Citharexylum spinosum*, J. Pharmacogn. Phytother. 2017, 173-184.
[22] F.K. El-Baz, A.Z. Hassan, H.I. Abd-Alla, H.F. Aly, K. Mahmoud, Phytochemical analysis, assessment of antiproliferative and free radical scavenging activity of *Morus alba* and *Morus rubra* fruits, Asian J. Pharmaceut. Clin. Res. 2017, 189-199.
[23] T. Mosmann, Rapid colorimetric assays for cellular growth and survival: Application to proliferation and cytotoxicity assays, J. Immunol. Methods 1983, 55-63.
[24] M.I. Thabrew, R.D. Hughes, I.G. McFarlane, Screening of hepatoprotective plant components using a HepG2 cell cytotoxicity assay, J. Pharm. Pharmacol. 1997, 1132-1135.
[25] A.F. Arafa, E.A. Younis, H.F. Aly, H. I. Abd-Alla, S.A. Ali, H.M. Sweelam, et al., Anti-amnesic effect of iridoids fraction from *Pentas lanceolata* leaves against D-galactose induced brain aging in rats, J. Glob. Pharma Technol. 2020, 464-473.
[26] T.L. Baker-Herman, D.D. Fuller, R.W. Bavis, A.G. Zabka, F.J. Golder, N.J. Doperalski, et al., BDNF is necessary and sufficient for spinal respiratory plasticity following intermittent hypoxia, Nature Neurosci. 2004, 48-55.
[27] T. Hirano, Interleukin 6 in The Cytokine Handbook, 3rd. ed. Academic Press, New York, 1998.
[28] D.L. Kasper, The polysaccharide capsule of *Bacteroides fragilis* subspecies *fragilis*: immunochemical and morphologic definition, J. Infect. Dis. 1976, 79-87.
[29] D.E. Kasper, M.E. Hayes, B.G. Reinap, F.O. Craft, A.B. Onderdonk, B.F. Polk, Isolation and identification of encapsulated strains of *Bacteroides fragilis*, J. Infect. Dis. 1977, 75-81.
[30] E.A. Badawy, W.I. Rasheed, T.R. Elias, J. Hussein, M. Harvi, S. Morsy, et al., Flaxseed oil reduces oxidative stress and enhances brain monoamines release in streptozotocin-induced diabetic rats, Hum. Exp. Toxicol. 2015, 1133-1138.
[31] K. Satoh, Serum lipid peroxide in cardiovascular disorders determined by a new colourimetric method, Clin. Chem. Acta. 1978, 37-42.
[32] H. Moshage, B. Kok, J.R. Huizenga, P.L.M. Jansen, Nitrite and nitrate determinations in plasma: A critical evaluation, Clin. Chem. 1995, 892-896.

[33] E. Beutler, O. Duron, B.M. Kelly, Improved method for the determination of blood glutathione, J. Lab. Clin. Med. 1963, 882-888.
[34] J. D. Bancroft, M. Gamble, Theory and practice of histological techniques. 6th Edition, Churchill Livingstone, Elsevier, China, 2008.
[35] R.M. Korany, K.S. Ahmed, H.A. Halawany, K.A. Ahmed, Effect of long-term arsenic exposure on female Albino rats with special reference to the protective role of *Spirulina platensis*, Explor. Anim. Med. Res. 2019, 125-136.
[36] N.M. Fayek, M.A. Farag, A.R. Abdel Monem, M.Y. Moussa, S.M. Abd-Elwahab, N.D.J. El-Tanbouly, Comparative metabolite profiling of four citrus peel cultivars via ultra-performance liquid chromatography coupled with quadrupoletime-of-flight-mass spectrometry and multivariate data analyses, Chromatogr. Sci. 2019, 349-360.
[37] H. Tsugawa, T. Cajka, T. Kind, Y. Ma, B. Higgins, K. Ikeda, et al., MS-DIAL: Data-independent MS/MS deconvolution for comprehensive metabolome analysis, Nat. Methods 2015, 523-526.
[38] H. Nawaz, M.A. Shad, N. Rehman, H. Andaleeb, N. Ullah, Effect of solvent polarity on extraction yield and antioxidant properties of phytochemicals from bean (*Phaseolus vulgaris*) seeds, Braz. J. Pharm. Sci. 2020, 1-9.
[39] S.B. Iloki-Assanga, L.M. Lewis-Luján, C.L. Lara-Espinoza, A.A. GilSalido, D. Fernandez-Angulo, J.L. Rubio-Pino, et al., Solvent effects on phytochemical constituent profiles and antioxidant activities, using four different extraction formulations for analysis of *Bucida buceras* L. and *Phoradendron californicum*, BMC Res. Notes 2015, 1-14.
[40] H.I. Abd-Alla, O. Kutkat, H.M. Sweelam, W.M. Eldehna, M.A. Mostafa, M.T. Ibrahim, et al., Investigating the potential anti-SARS-CoV-2 and anti-MERS-CoV activities of yellow Necklacepod among three selected medicinal plants: Extraction, isolation, identification, *in vitro*, modes of action, and molecular docking studies, Metabolites 2022, 1109.
[41] M. Bimakr, R.A. Rahman, F.S. Taip, A. Ganjloo, L.M. Salleh, J. Selamat, et al., Comparison of different extraction methods for the extraction of major bioactive flavonoid compounds from spearmint (*Mentha spicata* L.) leaves, Food Bioprod. Process. 2011, 67-72.
[42] T. Michel, E. Destandau, G. Le Floch, M.E. Lucchesi, C. Elfakir, Antimicrobial, antioxidant and phytochemical investigations of sea buckthorn (*Hippophaë rhamnoides* L.) leaf, stem, root and seed, Food Chem. 2012, 754-760.
[43] A.E. Allam, Antiallergic polyphenols from *Citharexylum spinosum*, Trends Phytochem. Res. 2017, 129-134.
[44] S.A. Saad, H.I. Abd-Alla, H.F. Aly, N.M.M. Shalaby, A.M.R. Afify, H.F.M. Ali, et al., *Citharexylum spinosum* promotes antioxidant, anti-inflammatory, and antiacetylcholinesterase activities. Egypt. J. Chem. 2024, 63-75.
[45] A.E. Allam, Stimulation of melanogenesis by polyphenolic compounds from *Citharexyllum quadrangulare* in B16F1 murine melanoma cells, Bull. Pharm. Sci. 2014, 105-115.
[46] M. Albini, A. Krawczun-Rygmaczewska, F. Cesca, Astrocytes and brain-derived neurotrophic factor (BDNF), Neurosci. Res. 2023, 11.
[47] M.P. Mattson, S. Maudsley, B. Martin, BDNF and 5-HT: a dynamic duo in agerelated neuronal plasticity and neurodegenerative disorders, Trends Neurosci. 2004, 589-594.
[48] Y. Liu, X. Fu, N. Lan, S. Li, J. Zhang, S. Wang, et al., Luteolin protects against high fat diet-induced cognitive deficits in obesity mice, Behav. Behav, Brain Res. 2014, 178-188.
[49] L. Zhao, J.L. Wang, R. Liu, X.X. Li, J.F. Li, L. Zhang, Neuroprotective, anti-amyloidogenic and neurotrophic effects of apigenin in an Alzheimer's disease mouse model, Molecules 2013, 9949-9965.
[50] Y.S. Li H.C., Ren, J.H. Cao, Roles of Interleukin-6-mediated immunometabolic reprogramming in COVID-19 and other viral infection-associated diseases, Int. Immunopharmacol. 2022, 1-16.
[51] L. Ferrucci, T. B. Harris, J. M. Guralnik, R.P. Tracy, M. C. Corti, H. J. Cohen, et al., Serum IL-6 level and the development of disability in older persons, J. Am. Geriatr. Soc. 1999, 639-646.
[52] H.F. ALY, H.I. Abd-Alla, S.A. Ali, R.A. Alez, T. Abu-Krisha, M.M. Mamdouh, Bioinformatics: inflammatory cytokines and attenuation of diabetes hypercholesterolemia-induced renal injury using morning glory and necklace pod extracts. Bioinformatics 2017, 347-355.
[53] M.H.H. Mohammed, A.N.E.S. Hamed, H.E. Khalil, M.S. Kamel, Phytochemical and pharmacological studies of *Citharexylum*

quadrangulare Jacq. Leaves, J. Med. Plants Res. 2016, 232-241.

[54] N.M.Shalaby, H.I. Abd-Alla, H.H. Ahmed, N. Basoudan, Protective effect of *Citrus sinensis* and *Citrus aurantifolia* against osteoporosis and their phytochemical constituents. J. Med. Plants Res. 2011, 579-588.

[55] C. Penido, K.A. Costa, D.O. Futuro, S.R. Paiva, M.A. Kaplan, M.R. Figueiredo, et al., Anti-inflammatory and anti-ulcerogenic properties of *Stachytarpheta cayennensis* (L.C. Rich) Vahl, J. Ethnopharmacol. 2006, 225-233.

[56] M.V.B. Monteiro, A.K.R. Leite, L.M. Bertini, S.M. Morais, D.C.S. Nunes-Pinheiro, Topical anti-inflammatory, gastro-protective and antioxidant effects of the essential oil of *Lippia sidoides* Cham. leaves, J. Ethnopharmacol. 2007, 378-382.

[57] U.B.S. Sorensen, K.H. Yao, Y.H. Yang, H. Tettelin, M. Kilian, Capsular polysaccharide expression in commensal *streptococcus* species: Genetic and antigenic similarities to *Streptococcus pneumonia*, MBIO 2017, 1-17.

[58] F.Y. Avci, D.L. Kasper, How bacterial carbohydrates influence the adaptive immune system, Annu. Rev. Immunol. 2010, 107-130.

[59] C. Ramakrishna, E.M. Cantin, IFN gamma inhibits G-CSF induced neutrophil expansion and invasion of the CNS to prevent viral encephalitis, PLos Pathog. 2018, 1-27.

[60] D.R. Chung, D.L. Kasper, R.J. Panzo, T. Chtinis, M.J. Grusby, M.H. Sayegh, et al., CD4+ T cells mediate abscess formation in intra-abdominal sepsis by an IL-17-dependent mechanism, J. Immunol. 2003,1958-1963.

[61] C. Liu, S. Zhang, H. Shi, H. Zhou, J. Zhuang, Y. Cao, et al., Atp11b deletion affects the gut microbiota and accelerates brain aging in mice, Brain Sci. 2022, 1-16.

[62] S. Zhu, Y. Jiang, K. Xu, M. Cui, W. Ye, G. Zhao, et al., The progress of gut microbiome research related to brain disorders, J. Neuroinflamm. 2020, 1-20.

[63] S. Filosa, F. Di Meo, S. Crispi, Polyphenols-gut microbiota interplay and brain neuromodulation, Neural Regen. Res. 2018, 2055-2059.

[64] Y. Zhang, W. Yu, L. Zhang, M. Wang, W. Chang, The interaction of polyphenols and the gut microbiota in neurodegenerative diseases, Nutrients 2022, 1-16.

[65] I. Saidi, P. Waffo-Téguo, A.E.L. El Ayeb-Zakhama, F. Harzallah-Skhiri, A. Marchal, H. Ben Jannet, Phytochemical study of the trunk bark of Citharexylum spinosum L. growing in Tunisia: Isolation and structure elucidation of iridoid glycosides, Phytochem. 2018, 47-55.

[66] H.I. Abd-Alla, D. Souguir, M.O. Radwan, Genus *Sophora*: a comprehensive review on secondary chemical metabolites and their biological aspects from achievements to future perspectives, Archiv. Pharmacal. Res. 2021, 1-84.

[67] B.M. Morsy, M.A. Hamed, H.I. Abd-Alla, W.M. Aziz, S.N. Kamel, Down regulation of fibrosis and inflammatory signaling pathways in rats liver *via Pulicaria crispa* aerial parts ethanol extract, Biomarkers 2021, 665-673.

[68] M.Z. Rizk, D.M. Abo-El-Matty, H.F. Aly, H.I. Abd-Alla, S.M. Saleh, E.A. Younis, et al., Therapeutic activity of sour orange albedo extract and abundant flavanones loaded silica nanoparticles against acrylamide-induced hepatotoxicity, Toxicol. Rep. 2018, 929-942.